

R8



UNIVERSITÀ DEGLI STUDI DI FIRENZE

DIPARTIMENTO
DI
INGEGNERIA ELETTRONICA

**Neural networks for the real time classification
of weld defects from ultrasonic data**

L. Capineri

Report N.931101 November 1993



Index

1. Introduction	3
2. Collection and preprocessing of ultrasonic data	5
3. Classification methods directly from ultrasonic raw data	11
3.1) Conventional pattern matching	12
3.2) The Adaptive Receptive Field method	13
3.3) The standard back propagation method	13
3.4) Hybrid methods involving receptive fields and back propagation	14
3.5) The shared weights back propagation method	15
4. Defects classification with neural networks	16
5. Real time classification and experimental set-up	20
6. Results of the classification on real defects	22
7. Conclusions	23
8. Acknowledgments	24
9. References	24

1. Introduction

The ultrasonic techniques are being widely used in the non-destructive testing field for flaw sizing and classification in metals. Flaw sizing has been solved by the ultrasound scattering theory that correlates the information contained in the received ultrasonic signals to the scattering properties of the flaws in the metal specimen [1]. This has been possible thanks to the great amount of research work in the ultrasonic scattering theory and reliable investigation techniques are now available for this scope [2]-[3].

On the other hand the classification of defects from ultrasonic images it's a matter of experience and confident evaluations are obtained only by well trained technical people.

Recently the problem of flaw classification has been tackled by several authors. In particular basic research works concerning the investigation of weld defects are carried out by Burch et al.[4] and Windsor et al.[5] and Windsor [6]. In the former work four classes of defects were defined: the classification of artificial defects was carried out by pattern recognition methods based on extracted features from the ultrasonic signals. The chosen type of defects significant for non-destructive testing of welds are: (i) smooth cracks; (ii) rough cracks; (iii) slag; (iv) porosity.

The choice of these classes is based on the risk factor associated to each type of defects: the cracks split in the first two classes are more critical than the regions of porosity or the lump of inhomogeneities.

The selection of meaningful features was not trivial in [4] and very good suggestions came from the experience learnt by the technical people during several years.

In the first approach with conventional classifiers were obtained interesting results but the discrimination between classes was not enough to get reliable responses. An improvement of the performances was attempted by replacing the conventional classifiers with neural network methods. Recently the neural networks received a broad acceptance and they are currently employed in several fields such as speech processing [19]-[20] and seismic data inversion [21]. Their success is due to the ability of giving correct answers with more generic situations presented at the inputs of the network and not less important the fast processing time.

The performances of the neural methods were compared with the classification of the set of

artificial buried defects used by Burch [4]. It turned out that the performances of the neural network classifier in the feature space were comparable to conventional ones. In particular the method of error back-propagation for training with a multi-layer fully connected network [18], did better than the Hopfield network. Despite of the faster non-iterative training procedure of the Hopfield method, this method has the drawback that points close together in the feature space do not necessarily correspond to images with many common points.

Thus from the results of the classification in the feature space emerges that exist good classifiers among conventional and neural methods, and a high success rate can be achieved when the classifiers are trained with significant set of features and consistent training samples. However the classification in the feature space revealed two main drawbacks in our applications:

- 1) *Too long computation to extract features: then the benefits of a fast classification offered by the neural networks are swamped because the computational task to derive a set of feature values demands powerful computers to get a real time response;*
- 2) *The subjective judgment is still needed to define the best set of features to be extracted from the ultrasonic images.*

Recent developments in artificial neural networks offer an alternative solution to this problem. Though these methods claim to be successful in many different applications, there are no elegant prescriptions that insure the success in the specific application.

Limiting the interest to supervised learning of clusters in n-dimensional feature space, there are several neural network architectures to be investigated for the present problem.

These points have suggested the investigation of new methods and here is proposed the automatic classification of weld defects directly from the ultrasonic images.

The classification of defects directly from the ultrasonic raw data has the advantage to be faster than the classification in the feature space because is not necessary the preliminary task of features calculation. Again both conventional and neural methods are considered but they have been adapted to our application that requests methods able to extract significant features and

classify.

However this report has devoted a special emphasis to neural methods, which are also the objectives of the european collaborative project ANNIE (Applications of Neural Networks for Industry). A preliminary analysis of different neural network methods [16]-[18] was carried out by the project ANNIE itself.

Many neural network methods that could be applied to the present problem of supervised learning of clusters in a n-dimensional feature space, have been reviewed by Grossberg [7], and by the ANNIE project itself [8]. Work in progress of this project are now addressed to the automatic classification of defects directly with ultrasonic images.

Then the obtainable performances and speed of the different classifiers were evaluated with the original dataset [4] and with new samples. The latter are gathered with a new experimental system designed for the assessment of defects in V welds and the results with three and four dimensional images are reported.

Probabilistic neural networks are an alternative solution to classify defects in welds by the ultrasonic monodimensional signals and recent results are reported by Song et al. [25].

2. Collection and preprocessing of ultrasonic data

Since our classification method is based on ultrasonic images instead of single A-scans, this section describes the characteristics and the requirements of the ultrasonic data collection and preprocessing of the raw ultrasonic images. After these operations a tied-up version of the input ultrasonic image is provided for the subsequent classification.

Investigations on the reflected signals from various type of defects, revealed that additional information of the defect type could be obtained with the analysis of the backscattered signals from the entire volume of the defect and over different inclinations. This means that is necessary to use three or four dimensional images, where the third dimension is the depth of the defect beneath the plane of the receiving aperture, and the fourth dimension is the angle of the incident ultrasound beam. By software the three dimensional (3D) images were formed by stacking a set of parallel B-scan acquired at different position along the weld direction (see figure 1).

The fourth dimension is provided by the acquisition with different probe angles. A data set with of four dimensional image of real defects was collected by Burch et al.[4]. In that work the defects of known type were introduced artificially into metal test pieces. The data took the form of three-dimensional ultrasonic reflected intensity as a function of position x, and y and depth z in the material. The four dimensional images were collected at two different angles, usually 0 and 20 degrees.

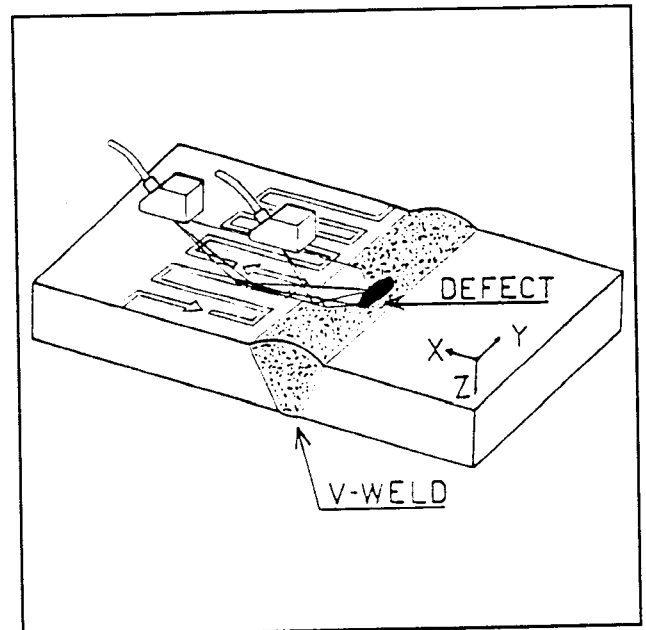


Figure 1 Ultrasonic scanning system for three/four dimensional acquisition: the volume is formed by the B-scans compound.

A usual problem of pattern recognition is how much a classification method depends

on the format of the input image. Therefore, the experimental data were reduced to a standard format with a preprocessor before the classification. Further details of the preprocessing influence on the classification are reported in the next section.

The first step for setting up a classifier is the collection of a real dataset that is later used for training.

In this work are considered two types of steel blocks containing artificial buried defects and the system for data collection is adapted to cope with the different defect scattering geometries: - in the first type the defects are at a given depth from the top surface and the direct pulse-echo reflected signals was acquired at 0° and 20° from the vertical. The measurements were carried out with a single immersion probe above the defect, coupled by water to the metal specimen (see figure 2a).

- in the second series the defects along V welds were considered and the backscattered signals was measured indirectly from the back wall of the plate sample (one or double ship inspection). Here we use contact probes with two different inclinations: 60° and 45° or 70° respectively (see figure 2b).

The inspection geometry has consequence on the treatment of these data, because the

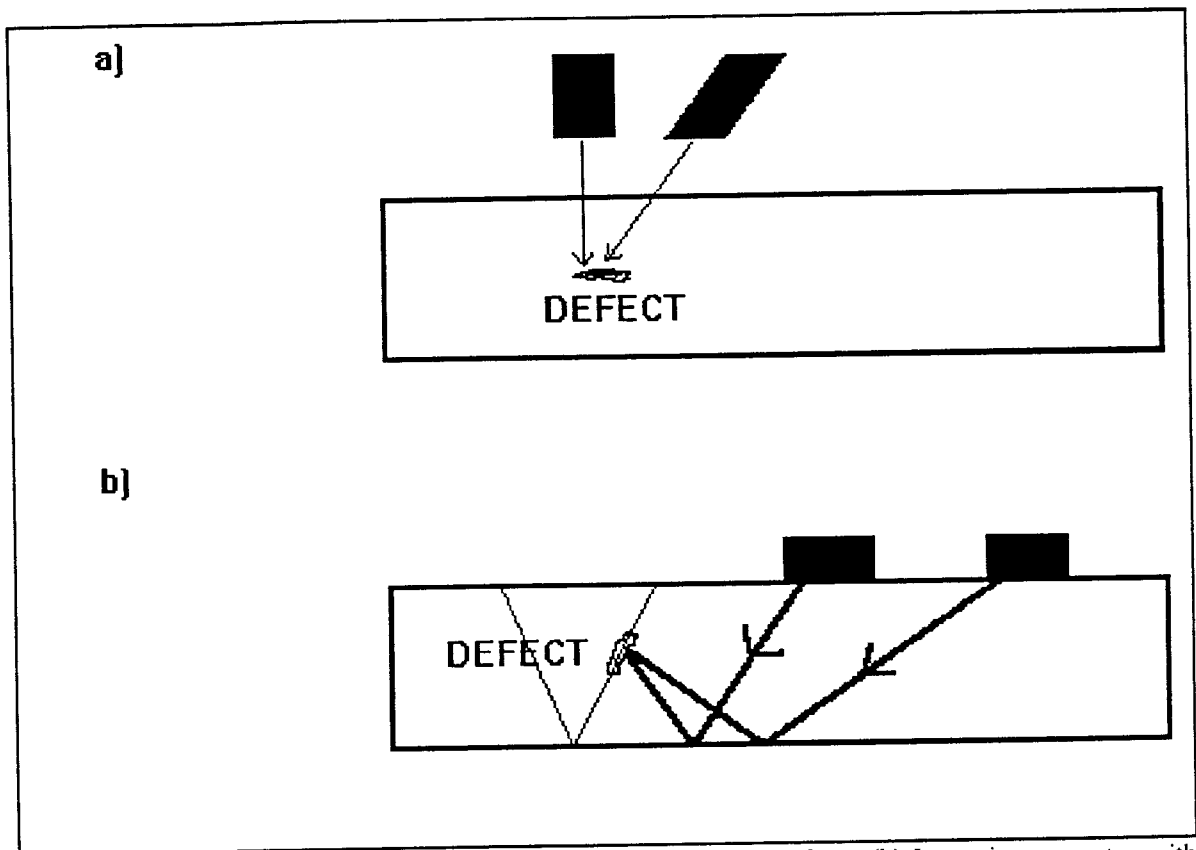


Figure 2 (a) Inspection geometry with immersion probe on planar defects. (b) Inspection geometry with angle contact probes for V welds with bottom wall reflection (one skip).

ultrasound propagation changes with the two different set-ups. In fact the signal amplitudes depend on the round trip path length as well the angle dependent reflections at the interfaces. The experimental implications on the classification performances are reported in section 5. Thus we normalised the signal amplitudes to compensate for different attenuations, by referring all the signals to those obtained from a calibration reflector such as a side drilled hole at fixed probe distance. Additional difficulties are due to the different sizes and resolutions of the experimental measurements.

From the above considerations a preprocessor program was developed to create a set of normalized data in a standard format to be presented to the classifier.

The first task of the preprocessor consists in places the original image onto an image of standard size, with the most appropriate resolution. In figure 3 there is an example of preprocessing for a two dimensional image: the three processes of centering, placing and

averaging carried out by the preprocessor.

The centering operation is based on the definition of the centre of gravity of the original image. Once this characteristic point is found, the original image is moved to a new standard size image with its center onto the centre of gravity. From experimental observations we found that the centre of gravity is better estimated by the data of the first angle probe. In fact the second probe provides low signal to noise images for non perpendicular incidence on the weld.

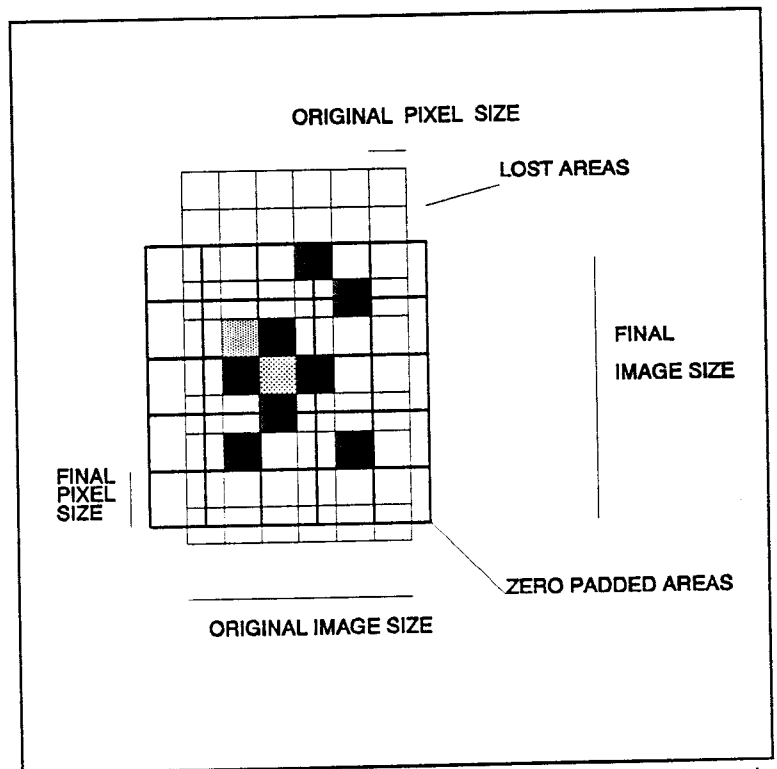


Figure 3 Averaging and centering task of the original ultrasonic image (raw data) for the two dimensional case.

The integration is made over both angles so that the center of gravity X_g, Y_g, Z_g of the four dimensional image $I(x,y,z,\alpha)$ is defined by the relationship (1) :

$$X_g = \frac{\sum_{x,y,z,\alpha} I(x,y,z,\alpha) x}{\sum_{x,y,z,\alpha} I(x,y,z,\alpha)} \quad (1)$$

and similarly for Y_g and Z_g .

The centre of gravity is then rounded to the nearest pixel. The next operation is to place a square scratch array of standard size of the image with the central pixel overlapped to the centre of gravity of the original image. Ideally the new images are symmetric respect to the centre of gravity if the array dimension is odd. Without loss of generality we have restricted our software to work with odd dimensional arrays.

Areas of the original image not contained by the new array are truncated and wasted. Areas of the new image that are not filled by the original image are zeros padded.

Generally the placing process is repeated because some parts of the original image are lost and the new centre of gravity may need to be recalculated until convergence. The averaging process generates a final image with the pixel size that is greater than the original ones. The average size is generally different along the cartesian axis to adjust different original resolutions of the collected data. Again the centre of gravity is hold in the central pixel if an odd average size is chosen. The optimum size of the averaging volume should be the largest as possible that preserves the essential features of the image to be correctly classified.

The last operation of the preprocessor is the amplitude normalization. The ultrasonic amplitude that we relied on, is the result of the rectification of digitized radiofrequency signal. As in other image analysis problems, here is assumed that only the image intensity distribution retains the essential features and the phase information is neglected. The absolute intensities of ultrasonic reflections were digitized onto 256 levels. However, this dynamics is further restricted by thresholding the data to provide a lower discrimination of significant defects. The lower level was set to 1% of the peak absolute intensity of each image. Then the peak intensity of each image was normalized to a constant value equal to 999. This method has the advantage that the images are experimentally consistent and they do not vary in intensity as the image size is changed. Alternative methods that normalize to a constant area of the image were also considered.

In figure 4 are reported with axonometric view the sample images of the ultrasonic response for each of four defect types in welds. The image size in figure 4 is $11 \times 11 \times 11 \times 2$ array, obtained from the preprocessing previously described of ultrasonic raw data. The figure shows the response from two different angles of ultrasound, with the probe angle at 0° (left), and 20° (right) to the vertical. The three elevations show the three integrals over the full data in the x, y and z directions. The height gives the intensity of the ultrasound reflection.

Section 3 of this report briefly illustrates the potential of automatic classification by different methods. In conclusion of this section it is interesting to spent some words on how the human can classify with their eyes from images such as in figure 4: the human expertise learns from its personal experience built up with the analysis of many images enclosing the expected range

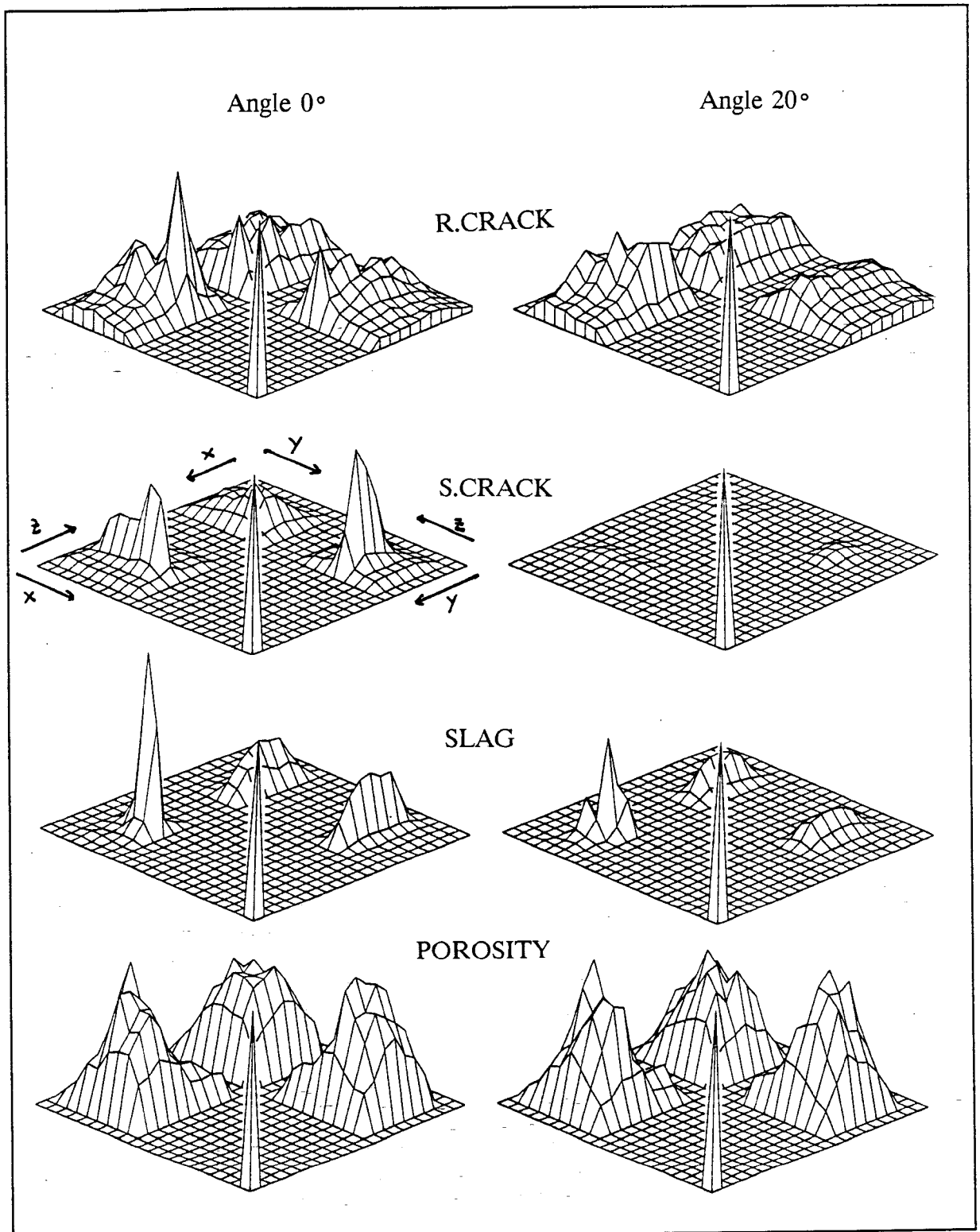


Figure 4 Pre-processed images of characteristics defects one for each type. Data are shown in axonometric view along the X,Y,Z reference system at angles 0° (left) and 20° (right).

of variations. Besides the case that some of them could be corrupted or incomplete data, these patterns are stored in the human memory and then used to assess new samples by matching or interpolating among the memorized prototypes. Concerning the case of ultrasonic defects classification, the humans can notice and extract gross and subtle features in the image intensities. What we normally do with our eyes, we scan across the image looking for relative heights, shapes and peak positions.

Moreover we can classify successfully whatever is the object position within the image since we operate on a topological context basis: in other words we need a classification invariant to the object transformation such as rotation and translation. As we will point out in the next sections a crucial point is the translational and rotational invariance of the classification methods.

3. Classification methods directly from ultrasonic raw data

The existing classification methods fall into two main categories: the statistical pattern recognition methods and the neural network based classifiers. Although the statistical classifiers are more general, the neural networks are more attractive for their speed and flexibility. The intrinsic parallel structure of the neural networks has a less computational complexity, which leads to fast response. However it's still unclear if the conventional pattern recognition will be replaced by the neural network approach and the debate is still open.

For specific problems definite indications for the choice of the best classification method can be achieved only after a systematic comparison of different methods.

Experience gained in real applications on both types of classifiers, has suggested the development of modified versions of the basic methods as well combination of different types. In the early stage of ANNIE project conventional pattern matching methods, neural network backpropagation and combination of both were analyzed. Some of them proven to fit for our goal giving a higher success rate in training and testing phase (say >90%).

Therefore the chosen methods used in this work are:

- 1) A conventional pattern matching method using prototypes for each class.

- 2) An adaptive field method in which receptive fields centred on peaks in the image are first extracted and averaged together to give a prototype for each class of the image.
- 3) Direct input to conventional back propagation neural network.
- 4) A receptive field input in which any field centred on a peak in the image becomes an example input to a back propagation net.
- 5) Direct input to the shared weights adaptation of the back propagation network.

Remanding the reader to the original works for the details on these methods [9]-[15], in the following are outlined their features and implications for the classification of defects in welds.

1) *Conventional pattern matching*

As an example of conventional image analysis methods, a standard pattern matching algorithm was applied to the four-dimensional data sets. In this method the training data set was used to define a single prototype or average image for each class. These four prototype images were stored and compared with each of the test images in turn. Considering the case of a two dimensional image (x,y) , if the prototype image for class c is described by $I_{c,x,y}$, and the test image for example e by the function $I_{e,x,y}$, then the pattern matching may be performed by evaluating the least squares difference:

$$D_c = \sum_{x,y} [I_{c,x,y} - I_{e,x,y}]^2 \quad (2)$$

The class with the minimum value of D_c then defines the class of the example.

The sums of the squares of the differences between corresponding pixels in each prototype and the test image is evaluated and the class with the lowest sum selected. The method was run in the average mode where the images of each class from the whole of the training set were averaged together. Since this method works essentially on template matching it is not translationally invariant. The centre of gravity placing of the image has provided an element of spatial invariance not unlike that given by the receptive fields considered later.

2) *The Adaptive Receptive Field method*

The reasons for the poor results using the conventional pattern matching method, relating to the conventional feature parameter classification methods are clear enough. Although the images had been roughly centred through their centre of gravity position, it remains a good deal of spatial variance in the position of the peaks and valleys in the image. The class significant relationships between adjacent pixels are smoothed out. Receptive field methods supply this spatial invariance by pattern matching on a smaller *receptive field* that is scanned across the image in a raster fashion. Briefly receptive fields are defined for each class. Initial receptive field values are defined from, for example, the positions in the image where there is a local peak. The receptive field is then refined iteratively by scanning over the training examples in each class and finding the position where the difference between the image and the field is a minimum. The portion of the image under the receptive field is then used to update the field of that class. In testing, each of the fields is scanned over the image in turn. The class whose field gives the best fit somewhere in the image is chosen.

3) *The standard back propagation method*

In the straightforward approach of the back propagation method each pixel in the image is presented as a separate input of the network. It is well known from a previous work on generic images and from many other studies [24], that the problem of this method is the disparity between the number of adjustable weights in the net and the number of distinguishable pixels in the data set. Therefore, from the above considerations the back propagation method can cope with multiple templates.

Although back propagation carries no direct information on the neighbourhood relationships between pixels in the image, these are implied indirectly through the training set. For example the smooth cracks correspond to a set of high values of adjacent pixels along a line in the image. The degree to which this information can be used by the method depends strongly on the number of training images.

4) *Hybrid methods involving receptive fields and back propagation*

Hybrid methods can be obtained by the combination of different standard classifiers and the resulting method takes advantage from the best characteristic of each one. A new method called the receptive field back propagation has been developed for our application.

There is a strong link between receptive fields and neural networks. Receptive fields detecting features such as orientated lines are known to exist in the visual cortex. The multiplicative field product is very similar to the sum of products of input vectors and weights of any neuron. Receptive fields may be classed as either "multiplicative" or "least squares". For example for a two dimensional image, the multiplicative field is computed by multiplying the portion of the image $I_{x,y}$ by the corresponding pixels in the receptive field $R_{x',y'}$. The summed products

$$P_c = \Sigma [I_{x,y} R_{x',y'}] \quad (3)$$

are noted. Here the best fit is given by the maximum response, or excitation value of the summed product P_c .

Because the scanning over the image can generally be done in parallel makes fast processing possible. The method of receptive fields is used by Fukushima in his neocognitron neural net model [22], and applied to character recognition. However, in the ultrasonic application the spatial positioning of the features is of very little utility. The neocognitron method has not therefore been pursued. The method used in this section was developed to combine the advantages of receptive fields with those of back propagation. The shared weights method may be considered to belong to this class of methods, but in general has been included in a separate section because of its wide acceptance.

The methods used in this section have all been developed for the present problem.

When a multiplicative receptive field for each class is used rather than a least squares field, a classification can in principle be made from that class with the maximum excitation product P_c . In practice this method has given poor results. Better results are obtained if the products P_c are treated as values in a feature space equal to the number of classes. Generally the back propagation and learning vector quantisation [17] have been used as classifiers in this work,

but the results obtained from other classifiers indicate that other choice are possible.

5) The shared weights back propagation method.

The shared weights development of the back propagation algorithm builds spatial invariance directly into the architecture of the network. The hidden layer weights are arranged in a two or three dimensional grid, as in the image, and may be considered as a receptive field. The connections from the image to the hidden layer are duplicated for every possible position of the hidden layer within the image. However the weights to the layer are not independent, but are constrained to a single set of values. The code used was that from the ANSim suite of neural network methods[26]. This technique proposed by Rumelhart in [18], has the advantage of few of parameters because many units share the same set of weights.

A preliminary work tested these algorithms on two dimensional artificial data sets [27]. The statistical features of the ultrasonic images of real defects were reproduced by a developed suite of software programs and most of synthesized ultrasonic images were created. This artificial dataset was employed for training and testing the above classifiers.

The adaptive least squares method (ii), the neural net receptive field back propagation method (iv), and the shared weights method (v) all gave good results comparable to those obtained in conventional feature extraction studies. The achieved results encouraged further developments and the results of the classification of three and four dimensional ultrasonic images of real defects are described in the rest of the paper.

4. Defects classification with neural networks

In this section we will discuss some questions related to the implementation of a classifier based on the two neural methods described in section 3.

Ideally, we would that the neural network classifier does what we do when we classify an image containing a defect: Therefore the neural classifier can extract and classify features automatically of the given input image.

The success rate in training and testing the network evaluates the performances and satisfactorily figures are often considered >90%.

The network performance is strongly influenced by the choice of the dataset and the lack of clear indications on this point lead very often to empirical solutions. One parameter that has to be set is the *learning fraction* p , defined as the fraction of the whole dataset for the training phase. The rest of the samples equal to $1-p$ will be used for testing.

Different values of p were tried but in the end the "Leave One Out" method was assumed. The LOO method is the conventional name for the procedure to be used when the learning fraction is nominally 100%. If all the data are available for training, a meaningful test success can be defined in which training is carried out using all the examples in the dataset except one. Testing is carried out only on this one example, and the process repeated until all examples in the dataset have been chosen. The overall success rate is then evaluated from the average over the results. The method is computationally intensive since the classification process is multiplied by the number of examples. However the method gives the success rate most appropriate to a commercial assessment, since it closely reflects the success rate of a new measurement made using all the existing data for training.

Another difficulty of neural network classifiers is the *overlearning* during the training phase. This problem is related with the net structure as well as its size. The size of the network defines the number of adjustable variables that are set during the training phase and then play an important role for overlearning. We can observe by the results obtained with conventional methods, that also these methods suffer of overlearning.

The *conventional pattern matching* method was tested with different input array size, from $11 \times 11 \times 11 \times 2$ to $5 \times 5 \times 5 \times 2$.

For all cases we obtained a best success rate around 86%, which is a rather indifferent performance especially when compared to that one obtained with the conventional pattern matching in the feature space. For the direct classification of ultrasonic images, the template matching suffers of the spatial variance in spite of the centre of gravity provides an element of spatial invariance. This means that the baricenter does not suffice to retain the essential features of each class: there are still remarkable variations in the relative positions of peaks and valleys of the images and consequently the essential features are smoothed out. This is not so for feature classification where the input variables can be assumed independent one of each others.

In the *adaptive receptive field* method, the scansion of the defect volume is done with a moving window, which works as a local feature extractor. If the size of the moving window is $3 \times 3 \times 3 \times 2$, there are at least 54 of adjustable variables equal to the number of the pixel in the receptive field. This is an advantage of this method over the standard back propagation as we will discuss later, because the problem of overfitting is unlike due to the reduced size of the adjustable variables. The results are less influenced by the number of the training examples and the choice of the learning fraction parameter, is less critical. In addition much of the optimization of the method could be performed with the otherwise artificial training set of all the available examples.

Among the neural methods we considered a fully connected net trained by the *direct back propagation algorithm*. In our implementations the image is directly presented as input field to the network. The size of the input image is much more crucial because the network learns from most of samples containing the different type of variance of the image. Thus, the results are strongly dependent from the number of training examples. Moreover, large input images lead to large difference between the number of adjustable weights and the number of distinguishable pixels in the image.

Therefore the original images of the dataset are averaged over a larger voxel: this operation reduces the size of the image but adjacent pixels can be correlated untruly. Considering the size of the averaged image equal to $7 \times 7 \times 7 \times 2$, and a network with two hidden units and four outputs, there are 1400 adjustable weights in the network. In this work the training

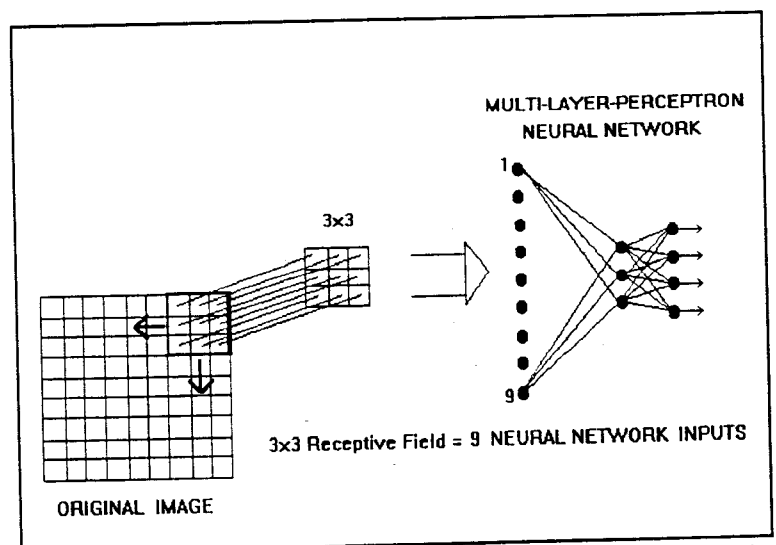


Figure 5 The receptive field method applied to neural networks: the input field selects a portion of the image with dimensionality smaller than the original one.

set consists of 66 samples of four dimensional images. It's evident the disparity between the number of input pixels (say $66 \times 7 \times 7 \times 7 \times 2 = 45276$) and the number of adjustable variables.

We have seen that with the direct back propagation method, the network is required to learn

the various types of variance present in the images. Large numbers of examples are required for this, and the consequently large networks make the results vulnerable to overfitting. The *hybrid methods* use a moving window rastered over the image, and the network has few inputs equal to the number of pixels within the window. The number of examples increases since the areas within several windows may be extracted from a single image. From the dataset of 11x11x11x2 images, the method produced a second dataset of say 3x3x3x2 window images, so that the field has the minimum size that allows the neighbour relationships to be examined. The window was instructed to pause at the position where the central pixel in the window was high, and intense enough to be at least half the maximum intensity in the image. These images were fed directly into a back propagation network as illustrated in figure 5. The devised method is less prone to overfitting because unlikely the backpropagation learns not generalized details from the multiplicative receptive field. As an example, assuming a network with four hidden units and four outputs the adjustable weights are 216 that are less than the standard back propagation.

Some results of this method applied to four defect types one for each class are presented in the tables 1.1-1.4. Different test conditions are considered: the receptive field stops on the portion of input image with highest central pixel (method MCP) and in another case where also the sum of outer pixels in the receptive field is maximum (method MSO); the method MCP is tested with different number of hidden units between 2 and 4.

Legend for tables 1.1-1.4:

-MCP Maximum Central Pixel, MSO Maximum Sum Outers

-Strikeout type is for misclassified case.

Table 1.1 Real defect is POROSITY					
# HIDDEN UNITS	Rec. Field METHOD	CLASS 1 POROSITY	CLASS 2 SLAG	CLASS 3 S.CRACK	CLASS 4 R.CRACK
2	MCP	0.000	0.039	0.0005	0.60
3	MCP	0.989	0.005	0.001	0.01
4	MCP	0.98	0.006	0.0006	0.011
3	MCP&MSO	0.99	0.006	0.0006	0.013

Table 1.2 Real defect is SLAG					
# HIDDEN UNITS	Rec.Field METHOD	CLASS 1 POROSITY	CLASS 2 SLAG	CLASS 3 S.CRACK	CLASS 4 R.CRACK
2	MCP	0.92	0.00	3exp-6	0.86
3	MCP	0.003	0.51	0.006	0.48
4	MCP	0.029	0.57	0.006	0.41
3	MCP&MSO	0.023	0.011	0.0038	0.94

Table 1.3 Real defect is SMOOTH CRACK					
# HIDDEN UNITS	Rec.Field METHOD	CLASS 1 POROSITY	CLASS 2 SLAG	CLASS 3 S.CRACK	CLASS 4 R.CRACK
2	MCP	0.00	0.01	0.99	7exp-6
3	MCP	0.002	0.019	0.987	0.00006
4	MCP	0.025	0.021	0.986	0.00006
3	MCP&MSO	0.004	0.001	0.989	0.00029

Table 1.4 Real defect is ROUGH CRACK					
# HIDDEN UNITS	Rec.Field METHOD	CLASS 1 POROSITY	CLASS 2 SLAG	CLASS 3 S.CRACK	CLASS 4 R.CRACK
2	MCP	0.00	0.017	0.98	0.00024
3	MCP	0.021	0.0005	0.12	0.73
4	MCP	0.017	0.001	0.051	0.85
3	MCP&MSO	0.99	0.0022	0.0016	0.0065

Some observations can be made about the above results:

- the method MCP performed well with number of hidden units 3 and 4 while with only 2 hidden units the network size is too small,
- the smooth crack type defect is classified surely instead of others such as the slag type with outputs close to the rough crack type (compare columns 4 and 6 of table 1.2).

The classification time is in the order of few seconds on a processor i386sx 16MHz without math coprocessor nor source code optimization and it is at least five times faster than the adaptive receptive field method.

5. Real time classification and experimental set-up.

A demonstration system is built up for the automatic defects classification in V-welds in steel. The designed demonstration system exploits the hardware and software features of the ZIPSCAN system [23]. This is a flexible ultrasonic equipment that copes with different ultrasonic inspection situations. Both the hardware and software of the ZIPSCAN are adaptable to develop new applications. In this section we show the capabilities of real-time classification with two of the classification methods in section 4.

Among the five methods described in the previous sections we have chosen the Adaptive Receptive Field and the Receptive Field Neural Network with standard Rumelhart Back-Propagation, because they merge fast response times with good performances. Moreover the two methods have a complementary behaviour about the decision boundaries between classes: the minimum distance classifier is well suited when the boundary is, or is close to be linear; for arbitrary complex boundaries the neural network algorithms perform better.

Both the methods were trained and tested on a data base of well-known defects (steel test-objects with artificially introduced defects), with a successful classification rate around 94%. The database of four dimensional (4D) raw data images comprising the defect volume was formed previously. The defects were scanned with parallel B-scan (x,y) along the weld direction z and repeated with a two-angle probe system (α_1, α_2). Dealing with defects in V welds in ferritic steel with thickness about 30mm, shear wave angle probe can be used with incident angle in the range 45-60 degree because they have the advantage of a higher spatial resolution ($V_{\text{shear}} = 3100$ instead of $V_{\text{long}} = 5900$ in stainless steel 347).

The chosen inspection technique uses the reflection of the ultrasonic beam on to the metal plate bottom, allowing the inspection of the whole weld extension with a reduced ultrasonic round trip path and consequently a lower attenuation. However the shear wave method may generate mode converted signals due to the defect inclination, that must be eliminated carefully with a proper selection of the acquisition time window.

In the early stage of this project a first prototype of on-line classifier was carried out for the classification of two dimensional images representing sections of the V-weld perpendicular to the weld direction. The results of the classification obtained with the former prototype system

outlined a poor discrimination between the porosity-rough crack defect and slag-smooth crack defect.

Therefore, the experimental results suggested expanding the system for the acquisition of four dimensional data to improve the success rate of the classification. A flexible acquisition system for up to 4D ultrasonic data has been designed and two classification programs have been modified to adjust the new dimensions of the input image for an on-line classification.

The acquisition of the ultrasonic signals reflected from a volume containing the defect, has some advantages for the classification, because each defect type has own well-defined features considering its expansion in three dimensions. In particular for the smooth crack and rough crack classes are better discriminated using the reflected signals over two different incident angles. Therefore the upgraded classifying system includes the signal acquisition from a second angle probe. In the new prototype the acquisition is completely computer controlled apart a manual movement in the weld direction. This movement will be controlled by the same computer in a forthcoming PC386 version by a robotized arm. The acquisition parameters such as spatial step, number of A-scans and B-scans are read in with a Fortran program by a Menu Driven System (MDS). During the acquisition the program gives information to the operator about the automatic and manual operations in progress. After the acquisition of the single B-scan, the detected image is transferred to a file on the ZIPSCAN virtual memory that accumulate all the images. Later the user can decide whether the data file with compatible ZIPSCAN format must be stored on the hard disk to create a data base of real defect images. Then the acquisition program changes the angle probe by resetting the movements to the initial position and the acquisition is repeated with a different incident angle.

Since the two data sets are obtained with different ultrasonic angle probes, it has been necessary to execute a run time system calibration when the two angle probes are exchanged. The two probes were calibrated by V1 type calibration blocks and the calibration parameters stored in a file.

6. Results of the classification on real defects

Finally the on line classifier was tested with real defects consisting of one defect for each type in a 60° V weld. The 4D images were acquired with the laboratory system described in section 5 and then reduced to a standard format with the preprocessing programs amended to treat 4D ultrasonic data sets. As previously described the task of the ultrasonic data preprocessing consists of the following operations:

- Centering by the evaluation of the center of gravity
- Normalization and thresholding
- Averaging on a defined volume and voxel size

Usually the size for of the processed image was chosen 11x11x11x2 but in our case we used 11x5x11x2 and 2x2x2 mm voxel size. Two contact shear wave probes with 4 MHz central frequency and incident angle 60° for the first probe, while the second angle probe was 45° or 70° depending on the position of the region to be inspected.

Preliminary results obtained with the adaptive receptive field classifier on a limited number of tests are reported. For each class of defect (porosity, slag, smooth and rough crack) a characteristic field with dimension 3x3x3x2 has been calculated with the data base of planar defects [28]. In turn each characteristic field is swept over the preprocessed image and the minimum distance between the characteristic field and the real image is calculated. Finally the class is chosen for the best match with the minimum distance criterion among the four classes. A first trial with 38 real samples gave a success rate of 73% that is worst than that obtained in the testing phase of about 94%. Further investigations on the misclassified cases showed that the intensities of the original images of both angles, didn't match the model of the receptive field used for the classification: in some cases the second probe (45°) signals were too high due to the higher amplification compared with the first probe and shorter ultrasonic path. The above experimental observations suggest using proper gain difference between the two angle probes for data acquisition.

The performances are improved further with a calibration procedure based on a ideal isotropic

reflector (say side drilled hole). The calibration is done at different ranges to count for the attenuation of ultrasound. Moreover we considered the different probe efficiency and the correction necessary for refraction due to the probe height [29]. It's worth to observe that this problem was negligible in the original data base acquired with planar defects and a single immersion probe tilted at different angles (see scanning geometry in Fig.2a).

We increased the versatility of the prototype system with the addition of a third contact 4 MHz - 70° shear wave probe. This probe can be activated directly by the operator with the MDS program interface for inspections of defects near the weld root.

After the amplitude correction the quality of the images has been improved and the defect features are better defined. The results of the classification of four real defects belonging to the 38 images data set are shown in Table 2.

Table 2. Results of the classification with the adaptive receptive field and amplitude calibration. Input image size 11x5x11x2, voxel resolution 2x2x2 mm.

Defect type	Gain difference compensation [dB]	Angle of contact probes	Defect range [mm]	Output 1 class (Porosity)	Output 2 class (Slag)	Output 3 class (Smooth Crack)	Output 4 class (Rough Crack)
Porosity	-2	60°-45°	80-100	<u>546</u>	1098	1683	798
Slag	-3	60°-45°	66-100	92	<u>75</u>	103	81
Smooth Crack	-2	60°-45°	80-112	1267	556	<u>112</u>	930
Rough Crack	+4	60°-70°	86-55	809	1208	1012	<u>553</u>

In Table 2 the correct responses are underlined. These results indicate an improved discrimination among the classes respect of the previous classifications with the corresponding uncompensated images. The following work is addressed to the application of this method the whole set of 38 sample images to reduce the number of misclassified cases.

7. Conclusions

The first part of this report examines the feasibility of conventional and neural network based classifiers and the relative merits for the defect classification with ultrasonic images. Among different classification methods, the direct classification from three dimensional ultrasonic images with neural network classifiers offers a new opportunity for a fast and automatic

- [4] BURCH S F and BEAUNG T N K, A physical approach to the automated ultrasonic characterization of buried weld defects in ferritic steel, NDT International, 19, 145-153 (1986)
- [5] Baker A R and Windsor C G, The classification of defects from ultrasonic data using neural networks: the Hopfield method, NDT International 22, 97-105 (1989)
- [6] Windsor C G, Neural Networks from Models to Applications, ed. Personnaz and Dreyfus, IDSET,

Firenze 8 Novembre 1993

Alla Procura della Repubblica di Firenze

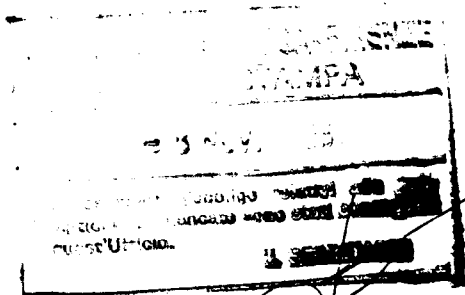
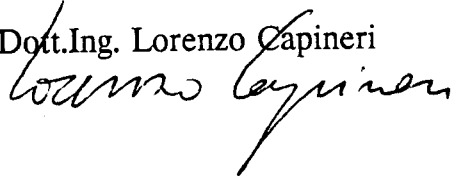
Si consegna a norma delle vigenti disposizioni di legge una copia del report interno N. 931101 del Dipartimento di Ingegneria Elettronica, Università degli Studi di Firenze a cura degli autori sotto elencati.

Titolo : Neural networks for the real-time classification of weld defects from ultrasonic data

Autori : Dott.Ing. Lorenzo Capineri

In fede

Dott.Ing. Lorenzo Capineri



Firenze 8 Novembre 1993

Alla Prefettura di Firenze
Ufficio Stampa

Si consegna a norma delle vigenti disposizioni di legge quattro copie del report interno N.931101 del Dipartimento di Ingegneria Elettronica, Università degli Studi di Firenze a cura degli autori sotto elencati.

Titolo : Neural networks for the real-time classification of weld defects from ultrasonic data

Autori : Dott.Ing. Lorenzo Capineri

In fede

Dott.Ing. Lorenzo Capineri

